EXTRACTING THE CHANNEL ALLOCATION INFORMATION IN A SPECTRUM POOLING SYSTEM USING CYCLIC FEATURE DETECTION

Mengüç Öner and Friedrich Jondral

Universität Karlsruhe, Institut für Nachrichtentechnik
D-76128 Karlsruhe, Germany
e-mail: oner@int.uni-karlsruhe.de

ABSTRACT

Spectrum pooling is a resource sharing strategy, which allows a license owner to share a sporadically used part of his licensed spectrum with a renter system, until he needs it himself. For a frictionless operation of a spectrum pooling system, the license owner has to have the absolute priority to access the shared spectrum. This means, the renter system has to monitor the channel and extract the channel allocation information (CAI), i.e. it has to detect, which parts of the shared spectrum the owner system accesses to, in order to immediately vacate the frequency bands being required by the license owner and to gain access to the frequency bands, which the license owner has stopped using. This paper proposes using cyclic feature detection for the extraction of the CAI in a specific spectrum pooling scenario, where the license owner is a GSM network and the spectrum renter is an OFDM based WLAN system.

1. INTRODUCTION

The spectrum pooling concept, which has been investigated in [1] and [2] can be considered as a first step towards a fully dynamic demand oriented spectrum allocation strategy. In [2], an OFDM based spectrum pooling system has been proposed, which makes it possible for the spectrum renter to adapt the number and the position of the modulated carriers according to the channel allocation information (CAI), i.e. the channel occupation of the license owner, thus minimizing the impact of the renter system on the operation of the owner system. In [2] , the CAI is extracted from the channel at regular intervals, during the so called silent periods, in which the renter system stops transmitting and performs energy measurements to detect the presence of the owner system in the channel. The energy detection approach requires the introduction of the silent periods, since this method is unable to discriminate between the signals of the owner and renter systems, and it has a poor reaction speed, because no detection is possible between two silent periods. To be able to monitor the CAI continuously, algorithms are required, which are capable of discriminating between the two signals and of detecting the presence of the owner signal even under the interference from the renter signal in the same frequency band. This paper investigates a specific spectrum pooling scenario which has a GSM network as the license owner and a wireless LAN system based on OFDM as the spectrum renter, as shown in Fig.1. Fig.2 illustrates a possible channel occupation of the proposed spectrum pooling system at a given time. In our paper, we propose exploiting the cyclostationary properties of the license owner signal to extract the CAI from the channel. We employ a cyclic feature detector to detect GSM-specific cyclic features at each GSM subband. Since the cyclic signatures of the OFDM based WLAN and GMSK modulated GSM signals differ significantly, this aproach allows the detection of the presence of the owner signal in the channel under severe interference from the renter signal. A detailed discussion about cyclostationarity and cyclic detectors can be found in [3].

2. CYCLOSTATIONARITY

Cyclic feature detection exploits the cyclostationary properties, which exists in most man-made communication signals, providing

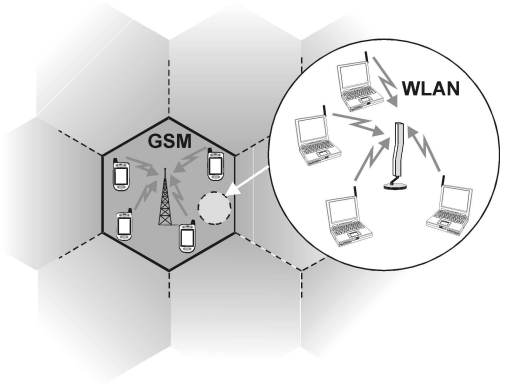

Figure 1: The spectrum pooling scenario under consideration. The license owner is a GSM network and the spectrum renter is a OFDM based WLAN system.

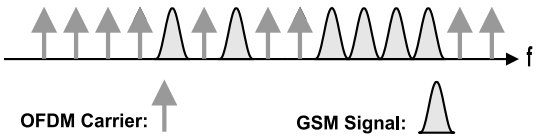

Figure 2: A possible channel occupation of the spectrum pooling scenario under consideration

improved presence detection performance compared to simple energy detection methods. The main advantage of the cyclic feature detection is its discriminatory capability. Since the cyclostationary properties of different signals are usually unique, distinct cyclic signatures can be used to separate the signals, even if they overlap in the frequency domain.

A signal $x(t)$ is called cyclostationary, when its time varying autocorrelation function $R_{xx}(t,t+\tau) = E\{x(t)x^*(t+\tau)\}$ is periodic in time t and admits a fourier series representation

$$R_{xx}(t,t+\tau) = \sum_{\alpha} R_{xx}^{\alpha}(\tau) e^{j2\pi\alpha t} \tag{1}$$

where the sum is taken over integer multiples of fundamental frequencies α. The fourier coefficients, which depend on the lag parameter τ can be calculated as

$$R_{xx}^{\alpha}(\tau) = \lim_{T\to\infty} \frac{1}{T} \int_{-T/2}^{T/2} R_{xx}(t,t+\tau) e^{-j2\pi\alpha t} dt. \tag{2}$$

With the assumption of cycloergodicity [3], this expression reduces to

$$R_{xx}^{\alpha}(\tau) = \lim_{T\to\infty} \frac{1}{T} \int_{-T/2}^{T/2} x(t)x^*(t+\tau) e^{-j2\pi\alpha t} dt. \tag{3}$$

$R_{xx}^{\alpha}(\tau)$ is called the cyclic autocorrelation function, and is continuous in τ but discrete in cycle frequency α. For $\alpha = 0$, it reduces

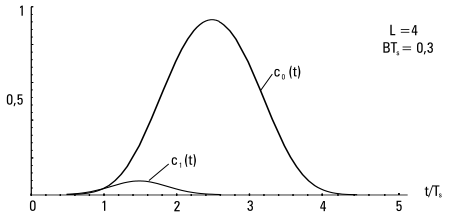

Figure 3: $c_0(t)$ and $c_1(t)$ for $L = 4$, $BT_s = 0.3$

to the conventional autocorrelation function $R_{xx}(\tau)$. For a signal which does not exhibit cyclostationary, $R^{\alpha}_{xx}(\tau) = 0, \forall \alpha \neq 0$. The Fourier transform of the cyclic autocorrelation function

$$S^{\alpha}_{xx}(f) = \int_{-\infty}^{\infty} R^{\alpha}_{xx}(\tau) e^{-j2\pi f\tau} d\tau. \tag{4}$$

is called the spectral correlation density, which can be seen as a generalization of the conventional power spectral density function. A useful modification of the cyclic autocorrelation function is obtained by deleting the conjugate in the lag product

$$R^{\alpha}_{xx^*}(\tau) = \lim_{T\to\infty} \frac{1}{T} \int_{-T/2}^{T/2} x(t)x(t+\tau)e^{-j2\pi\alpha t} dt. \tag{5}$$

This modification is called the conjugate cyclic autocorrelation function. The conjugate spectral correlation density function $S^{\alpha}_{xx^*}(f)$ is defined similarly:

$$S^{\alpha}_{xx^*}(f) = \int_{-\infty}^{\infty} R^{\alpha}_{xx^*}(\tau) e^{-j2\pi f\tau} d\tau. \tag{6}$$

Both the cyclic autocorrelation and the spectral correlation density functions (conjugate or nonconjugate) are discrete functions of the cycle frequencies α. The values of the α, for which these functions are are nonzero is determined by the hidden underlying periodicities found in $x(t)$ and constitute a unique cyclic signature for this signal. For communication signals, these cycle frequencies are typically related to the symbol rate and the carrier frequency. This cyclic signature can be exploited to detect the presence of a known signal under noise and interference. In the following sections, we are going to investigate the cyclic properties of a baseband GMSK (Gaussian minimum shift keying) modulated signal, in order to design an appropriate cyclic detector for the license owner system. To facilitate the analysis, we will separate the GMSK signal into its linear and nonlinear components, and focus on the linear component of the signal, which is a valid approach, since it contains about 99% of the signal power.

3. LINEARISATION OF GMSK

GMSK modulation, which is used in GSM, can be interpreted as a 2-level FSK modulation with a modulation index $h = 0.5$. The complex envelope of a GMSK modulated signal is

$$s(t) = exp\big[j2\pi h \sum_{n=-\infty}^{\infty} d_n \int_{-\infty}^{t} g(\tau - nT_s) d\tau\big] \tag{7}$$

with the symbol sequence $d_n \in \{-1, 1\}$, symbol rate $f_s = 1/T_s$and frequency impulse $g(t)$ given as

$$g(t) = \frac{1}{T_s} rect\big(\frac{t}{T_s}\big) * p_{Gauss}(t) \tag{8}$$

$p_{Gauss}(t)$ is a Gaussian impulse with the time bandwidth product BT_s. For the GSM system, the factor $BT_s = 0.3$ was chosen. In practice, the infinite long Gaussian impulse is cut to a length LT with $L \geq 3$. In [4], it is shown that a GMSK signal with $L = 4$ can be represented as the superposition of a linear and a nonlinear component:

$$\begin{aligned} s(t) &= \sum_{n=-\infty}^{\infty} exp\big[j\pi h \sum_{i=-\infty}^{n} d_i\big] c_0(t - nT_s) \\ &+ \sum_{n=-\infty}^{\infty} \sum_{K=1}^{7} exp[j\pi A_{K,n}] c_K(t - nT_s) \\ &= s^{lin}(t) + s^{nl}(t) \end{aligned} \tag{9}$$

where $A_{K,n}$ is a well defined function of the symbol sequence d_n and $c_K(t)$ are specific elementary impulse forms. In Fig. 3, the first two impulses $c_0(t)$ and $c_1(t)$ are displayed. It can be shown that $c_0(t)$ contains 99% of the signal energy. For a detailed discussion on this representation and the elementary impulse functions $c_K(t)$, see [4]. The linear part of the signal $s^{lin}(t)$ can be written as

$$s^{lin}(t) = \sum_{n=-\infty}^{\infty} z_n c_0(t - nT_s) \tag{10}$$

with the symbol sequence

$$z_n = j d_n z_{n-1} \tag{11}$$

Since the input signal sequence $d_n \in \{-1, 1\}$, we see that the sequence z_n consists of alternating real and imaginary symbols. This property results in a conjugate cyclostationarity of the GMSK signal, which is going to be investigated in the next section.

4. CYCLOSTATIONARY PROPERTIES OF A GMSK SIGNAL

We start our analysis with the conjugate cyclic autocorrelation $R^{\alpha}_{ss^*}(\tau)$ of a GMSK signal. In light of the discussion above, we are going to consider only the linear part of the signal. Assuming that the timing of the signal is unknown to the receiver, we can express the conjugate cyclic autocorrelation function due to the linear component of the signal as:

$$R^{\alpha}_{ss^*}(\tau) = \lim_{T\to\infty} \frac{1}{T} \int_{-T/2}^{T/2} s^{lin}(t+\varepsilon) s^{lin}(t+\tau+\varepsilon) e^{-j2\pi\alpha t} dt. \tag{12}$$

With the unknown symbol timing ε. In the following, we are going to find out the cycle frequencies, for which the GMSK signal exhibits conjugate cyclostationarity, and derive the expressions for $R^{\alpha}_{ss^*}(\tau)$. Looking at the lag product inside the integral of (12) $y(t) = s^{lin}(t+\varepsilon)s^{lin}(t+\tau+\varepsilon)$ more closely, we see that it contains a periodic component $y_{per}(t)$

$$\begin{aligned} y(t) &= \sum_{n=-\infty}^{+\infty} z_n c_0(t - \varepsilon - nT_s) \sum_{m=-\infty}^{+\infty} z_m c_0(t - \varepsilon - \tau - mT_s) \\ &= \sum_{n=-\infty}^{+\infty} \sum_{\substack{m=-\infty \\ m\neq n}}^{+\infty} z_n z_m c_0(t - \varepsilon - nT_s) c_0(t - \varepsilon - \tau - mT_s) \\ &+ \sum_{n=-\infty}^{+\infty} z_n^2 c_0(t - \varepsilon - nT_s) c_0(t - \varepsilon - \tau - nT_s) \\ &= y_{rand}(t) + y_{per}(t) \end{aligned}$$

$y_{per}(t)$ is nonrandom and periodic with a period of $2T_s$ because of the fact that z_n is a sequence of alternating real and imaginary

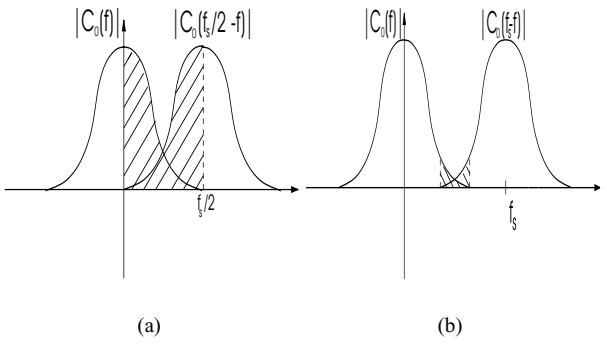

Figure 4: Spectral overlapping for (a) the conjugate and (b) the non-conjugate cyclic autocorrelation functions

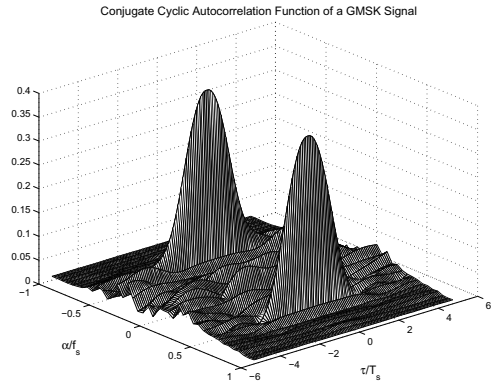

Figure 5: The magnitude of the conjugate cyclic autocorrelation estimate of a GMSK signal, data segment length $T_o = 500T_s$

symbols with unit magnitude (see (11)), which makes z_n^2 a sequence of alternating ± 1.We can write:

$$y_{per}(t) = \sum_{n=-\infty}^{+\infty} w(-1)^n c_0(t-\varepsilon-nT_s)c_0(t-\varepsilon-\tau-nT_s) \quad (13)$$

with the constant $w \in \{-1,1\}$. On the other hand, $y_{rand}(t)$ is random with no periodicity. Hence, the only contribution to $R_{ss^*}^{\alpha}(\tau)$ comes from $y_{per}(t)$ and for cycle frequencies which are integer multiples of $1/(2T_s)$, which leads to a conjugate cyclostationarity with cycle frequencies $\alpha = k/2T_s = kf_s/2$, $k = 1,2,3\ldots$ We can write

$$R_{ss^*}^{\alpha}(\tau) = \begin{cases} R_{ss^*}^{kf_s/2}(\tau), & \alpha = kf_s/2 \\ 0, & \text{otherwise} \end{cases} \quad (14)$$

The conjugate cyclic autocorrelation function can be calculated as

$$\begin{aligned} R_{ss^*}^{kf_s/2}(\tau) &= w \lim_{T\to\infty} \frac{1}{T} \int_{-T/2}^{T/2} \sum_{n=-\infty}^{\infty} (-1)^n c_0(t-\varepsilon-nT_s) \\ &\cdot \; c_0(t-\varepsilon-\tau-nT_s)e^{-jk2\pi(f_s/2)t}dt. \end{aligned} \quad (15)$$

Expressing $c_0(t)$ in terms of its Fourier transform $C_0(f)$ and using $(-1)^n = e^{j\pi n}$, we get:

$$\begin{aligned} R_{ss^*}^{kf_s/2}(\tau) &= w \lim_{T\to\infty} \frac{1}{T} \int_{-T/2}^{T/2} \int_{-\infty}^{\infty} \int_{-\infty}^{\infty} \Big[exp[j2\pi\big(f_1 t - f_1\varepsilon \\ &\quad + f_2 t - f_2\varepsilon - f_2\tau - k(f_s/2)t\big)]C_0(f_1)C_0(f_2) \\ &\cdot \; \sum_{n=-\infty}^{\infty} e^{-j2\pi nT_s[f_1+f_2-(f_s/2)]} \Big] df_1 df_2 dt. \end{aligned} \quad (16)$$

Expressing the infinite sum of phasors as an infinite sum of impulses we get

$$\begin{aligned} R_{ss^*}^{kf_s/2}(\tau) &= \frac{w}{T_s} \lim_{T\to\infty} \frac{1}{T} \int_{-T/2}^{T/2} \int_{-\infty}^{\infty} \int_{-\infty}^{\infty} \Big[exp[j2\pi\big(f_1 t - f_1\varepsilon \\ &\quad + f_2 t - f_2\varepsilon - f_2\tau - k(f_s/2)t\big)]C_0(f_1)C_0(f_2) \\ &\cdot \; \sum_{i=-\infty}^{\infty} \delta[f_1 + f_2 - f_s(i+\frac{1}{2})] \Big] df_1 df_2 dt. \end{aligned} \quad (17)$$

Integrating with respect to f_1 to eliminate the impulses leads to

$$\begin{aligned} R_{ss^*}^{kf_s/2}(\tau) &= \frac{w}{T_s} \int_{-\infty}^{\infty} e^{-j2\pi f\tau} C_0(f) \\ &\cdot \; \sum_{i=-\infty}^{\infty} C_0(f_s\frac{2i+1}{2} - f)e^{-j2\pi f_s\varepsilon\frac{2i+1}{2}} \\ &\cdot \; \lim_{T\to\infty} \frac{1}{T} \int_{-T/2}^{T/2} e^{j2\pi f_s t\frac{2i+1-k}{2}} dt df. \\ &= \frac{w}{T_s} \int_{-\infty}^{\infty} e^{-j2\pi(f\tau+\frac{k}{2}f_s\varepsilon)} C_0(f)C_0(k\frac{f_s}{2} - f)df \end{aligned} \quad (18)$$

From (18), we conclude that the energy contained in the $R_{ss^*}^{kf_s/2}(\tau)$ depends on the amount of the spectral overlapping between $C_0(f)$ and $C_0(k\frac{f_s}{2} - f)$, which is illustrated in Fig.4(a) for $k = 1$. Since the spectral overlapping is maximum for $k = 1$ the resulting cyclic correlation for $k = 1$ is obviously the strongest one. The magnitude of the conjugate cyclic autocorrelation function $R_{ss^*}^{\alpha}(\tau)$ of a GMSK signal with $BT_s = 0.3$ is shown in Fig.5, where the discrete cyclic correlation surfaces of the signal at $\alpha = \pm f_s/2$ are clearly visible.

It can also be shown, using a similar analysis, that the GMSK signal also exhibits nonconjugate cyclostationarity with a cycle frequency $\alpha = kf_s$. The cyclic correlation function can be calculated as

$$R_{ss}^{kf_s}(\tau) = \frac{1}{T_s} \int_{-\infty}^{\infty} e^{-j2\pi(f\tau+kf_s\varepsilon)} C_0(f)C_0(kf_s - f)df \quad (19)$$

Fig.4(b) illustrates the spectral overlapping between $C_0(f)$ and $C_0(kf_s - f)$ for $k = 1$. The spectral overlapping in this case is very small, leading to a very faint cyclic signature, which is much more difficult to detect under noise and interference. From this reason, we have chosen to exploit the conjugate cyclostationarity of the GMSK signal for the extraction of the CAI.

5. CYCLIC FEATURE DETECTION

The cyclic feature detector used in our paper detects the presence of the GMSK modulated signal exploiting its conjugate cyclostationarity at the cycle frequency $\alpha = f_s/2$. The detector operates by generating a decision statistics integrating the the frequency components of the conjugate spectral correlation density estimate $\hat{S}_{xx^*}^{\alpha}(f)$ of the received signal $r(t)$.

$$V(\alpha) = |\int_{-\infty}^{\infty} \hat{S}_{xx^*}^{\alpha}(f)df| \quad (20)$$

This detector is very similar to the single cycle detector proposed in [3] and in [5], the only difference being that we use the conjugate

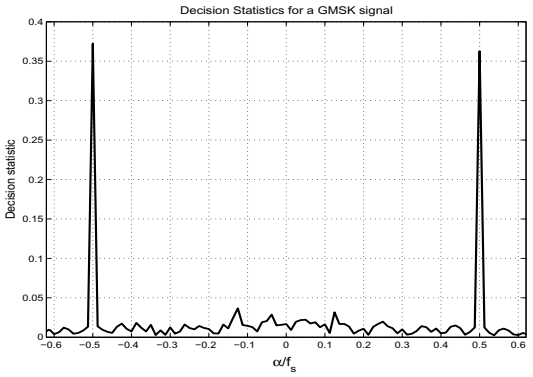

Figure 6: The decision statistics $V(\alpha)$ vs. α for a GMSK signal with $BT_s = 0.3$,

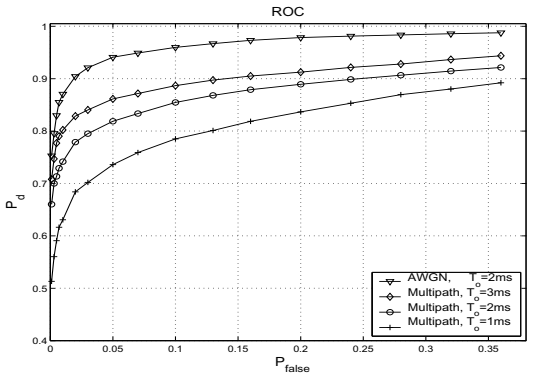

Figure 7: Receiver operating characteristics (ROC), SIR=0dB

spectral correlation density to form the decision statistics, instead of the nonconjugate one. In our work, $\hat{S}^{\alpha}_{xx^*}(f)$ has been estimated using a time smoothing method on a data segment of length T_o. Fig.6 shows the decision statistics for a GMSK signal with $BT_s = 0.3$ for different values of the cycle frequency α. As expected, the decision statictics $V(\alpha)$ exhibits maxima at the cycle frequencies $\alpha = \pm f_s/2$. For the decision making, we use an algorithm devised to detect the presence of those maxima.

6. SIMULATION RESULTS

In the following simulations, the license owner is a GSM system with a bandwith of 200 kHz per channel and a symbol rate $f_s = 1/T_s = 270.833$ kbit/s. The spectrum renter is an OFDM based WLAN system with 8 carriers and a carrier separation of 200 kHz, and uses QPSK modulation on each carrier. Both pure AWGN and frequency selective multipath fading channels are considered. In the latter case, we chose the typical urban channel model [6] for the GSM and Indoor B channel [7] for the WLAN system with user speeds of 5m/s. The signal to interference ratio SIR is defined as the ratio of the power of the GSM signal to the power of the interfering WLAN signal which falls into the same 200 kHz band. Fig.7 plots the receiver operating characteristics (ROC) of the proposed detector for a SIR of 0 dB and three different T_o for the multipath case. As a comparison, the ROC for a case without multipath propagation is also shown. The probability of detection P_d and the false alarm rate P_{false} are defined as:

$P_d = Prob(\text{GSM detected}|\text{GSM and WLAN are present})$

$P_{false} = Prob(\text{GSM detected}|\text{only WLAN is present})$

The results indicate a degradation in the performance of the detector due to the frequency selective nature of the multipath propagation channel. Increasing the length of the observation window

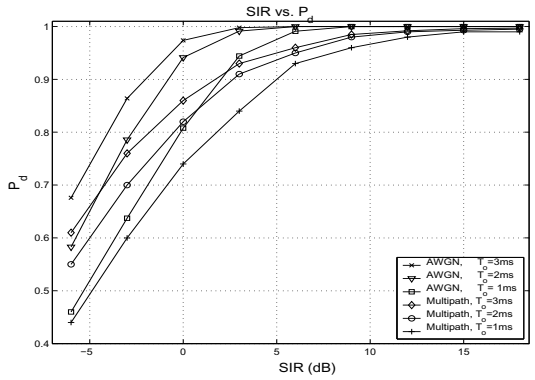

Figure 8: P_d vs SIR for $P_{false} = 0.05$

T_o leads to an increase in the performance of the detector, at the expense of reducing the reaction speed of the overall system. The same effects can be observed in Fig.8, where P_d vs. SIR for a fixed false alarm rate $P_{false} = 0.05$ is plotted. For the multipath case, which has more practical relevance, a satisfactory detection performance is achieved for SIR$\geq$ 3dB and $T_o \geq 2ms$.

7. CONCLUSION

We have demonstrated the use of cyclic feature detection in extracting the CAI in a spectrum pooling system where a GSM network is the license owner and a WLAN system is the spectrum renter. The proposed algorithm eliminates the need of silent periods and allows continuous channel monitoring. The simulation results indicate that a satisfactory performance can be achieved for SIR $\geq$ 3 dB. The overall detection probability of the spectrum pooling system can be further increased by using multiple cyclic feature detectors distributed inside the WLAN cell, which perform independent channel measurements. Determining the SIR levels which can be encountered in practice is a subject of further investigations.

REFERENCES

[1] F.Capar, I. Martoyo, T. Weiss, F. Jondral; "Comparison of bandwidth utilization for controlled and uncontrolled channel assignment in a spectrum pooling system" in *Proc. IEEE 55th Vehicular Technology Conference, Spring 2002*, vol.3, 2002 pp.1069-1073.

[2] F. Capar, F. Jondral, "Resource Allocation in a Spectrum Pooling System for Packet Radio Networks Using OFDM/TDMA", in*Proc. IST Mobile and Wireless Telecommunications Summit 2002*, Thessaloniki (Greece), June 2002, pp.489-493.

[3] W.A.Gardner, "Signal interception: a unifying theoretical framework for feature detection" *IEEE Transactions on Communications*, Volume: 36 , Issue: 8 , Aug. 1988 pp:897-906.

[4] A.Wiesler, R.Machauer, F. Jondral, "Comparison of GMSK and linear approximated GMSK for use in software radio", in *Proc.IEEE 5th International Symposium on Spread Spectrum Techniques and Applications* Sep 1998, vol.2, pp.557-560.

[5] Mills, R.F.; "Implementation of the single cycle detector using the signal processing workstation", in *Proc. Tactical Communications Conference*,10-12 May 1994 pp:393-400.

[6] COST 207: *Digital land mobile radio communications*, Commision of the European Communities, 1988.

[7] UMTS 30.03, Annex B: *Test environments and deployment models*, TR 101 1112, v.3.2.0, Apr. 1998.